The Effect of Bubbles Released from a Melting Ice Wall on the Melt-Driven Convection in Salt Water

EDWARD G. JOSBERGER

School of Oceanography, Oregon State University, Corvallis 97331

17 May 1979 and 22 October 1979

ABSTRACT

The buoyancy created by the release of air bubbles from melting glacial ice walls results from both the upward drag of the bubbles and the density defect caused by the steady-state distribution of bubbles in the water. Calculations using typical antarctic ice bubble concentrations and Southern Ocean temperatures and salinities show that the bubble buoyancy is comparable to the dilution for vertical ice length scales greater than 100 m. A comparison of laboratory experiments using 0.6 m long sheets of both bubbly and bubble-free ice shows two additional bubble effects. First, the bubbly ice melts in an irregular fashion that produces indentations in the ice which measure 20 mm long, 25 mm wide and 5 mm deep, while the bubble-free ice melts smoothly. Second, the ice-water interface salinity in the bubbly case is higher than in the bubble-free case. Finally, the observed melt rates lie within 10% of the observed melt rates from the bubble free experiments.

1. Introduction

When a vertical glacier ice wall melts in seawater, the buoyancy that drives the convection next to the ice is produced in two ways. The first is the cooling and dilution at the ice-water interface as described in Josberger (1979) and the second is the release of air bubbles from the melting ice. This study first derives an expression for the bubble concentration adjacent to a melting ice wall and then computes the additional buoyancy due to the bubbles which results from two effects: 1) the density defect created by the steady-state distribution of bubbles in the water and 2) the momentum imparted to the water by upward motion of these bubbles. Next, a laboratory experiment where vertical ice slabs with bubble concentrations comparable to glacier ice, melt in NaCl solutions at oceanic salinities and temperatures show two additional effects. The surface roughness which results from the bubbles in the ice increases the ice-water interface salinity and the ice no longer melts in the smooth fashion of the bubble-free ice experiments of Josberger (1979).

2. Bubble concentrations in glacier ice

The bubbles in glacier ice result from the metamorphosis of snow into ice. Patterson (1975) defines glacier ice as snow that has metamorphosed to the point where the snow is no longer porous or the individual air pockets are no longer connected to each other. At this depth which is called the firn line, the air pockets or bubbles are at 1 atm of pressure. Patterson gives air concentrations in ice as high as 7% by volume at atmospheric pressure.

In other measurements, Gow (1968) cored the antarctic ice cap at Byrd Station and reports an average bubble concentration of 0.22 bubbles mm^{-3} below the firn line at 64 m. This corresponds to an

0022-3670/80/030474-04$05.00

air concentration of 10% by volume. The diameters of the bubbles, which remained spherical, varied from 0.95 mm at 64 m to 0.33 mm at 279 m; the decrease in diameter results from the increased pressure at depth.

3. Steady-state bubble concentration

To determine the steady-state concentration of bubbles in the water adjacent to the ice, I assume all of the bubbles rise at their terminal velocity, the bubbles at any level have the same radius and there is no coalescence of the bubbles. Then, the divergence of the upward bubble flux in the water must equal the input of bubbles by wall melting. With z as the vertical coordinate, this is written as

$$\frac{d}{dz}(u_T N_w) = \sigma N_i, \tag{1}$$

where

σ melting rate
N_i bubble concentration within the ice
u_T terminal velocity of the bubbles
N_w integrated bubble concentration in the water.

Because Eq. (1) is a perfect differential, separation and integration gives

$$N_w = \frac{N_i}{u_T}\int_0^z \sigma dz, \tag{2}$$

for a uniform ice bubble concentration and a vertically varying melt rate.

Batchelor (1967) gives the terminal velocity of bubbles rising in a fluid as

$$u_T = \frac{r^2 g}{3\nu}, \tag{3}$$

where r is the bubble radius, g the acceleration of gravity and ν the kinematic viscosity. The terminal velocity is a function of depth because the bubble radius decreases with increasing hydrostatic pressure. For convenience, we define $\hat{p}$ as the nondimensional pressure given by

$$\hat{p} = \frac{p_1}{p}, \tag{4}$$

where p_1 represents atmospheric pressure and p is the pressure at depth. Then the ideal gas law gives the bubble radius at any depth as

$$r = r_1\hat{p}^{1/3}, \tag{5}$$

where r_1 is the bubble radius at 1 atm of pressure and r equals the bubble radius at depth. Table 1 gives $\hat{p}^{1/3}$ for an iceberg with a 200 m draft for $0 \leq z \leq 200$ m. Substitution of Eqs. (3) and (5) into (2) gives

TABLE 1. Pressure effect on bubble radius.

z	$\hat{p}^{1/3}$
50	0.40
100	0.45
150	0.55
175	0.66
200	1.00

$$N_w = \frac{3\nu N_1}{g r_1^2(\hat{p})^{2/3}}\int_0^z \sigma dz \tag{6}$$

for the steady-state bubble concentration in the water next to the ice.

4. Buoyancy computations

The buoyancy generated by each bubble in the water next to the ice results from two effects: 1) a bubble creates a density defect within the boundary layer, and 2) a bubble rising at terminal velocity exerts an upward buoyancy force on the surrounding water. This buoyancy force is balanced by a drag force, which is the second buoyancy effect. From Eq. (6), the buoyancy force on each bubble at any depth is

$$B = \frac{4\pi}{3}\rho_w g r_1^3\hat{p}. \tag{7}$$

Multiplication of Eq. (7) by wN_w/ρ_w gives the total buoyancy effect as

$$B = 8\pi r_1 \nu N_1 \hat{p}^{1/3}\int_0^z \sigma dz. \tag{8}$$

5. The dilution buoyancy

The buoyancy generated by a melting ice wall in salt water and integrated over the width of flow is

$$B_d = g\int_0^\infty \frac{(\rho_\infty - \rho)}{\rho_\infty}dy, \tag{9}$$

where B_d equals the integrated buoyancy and ρ_∞ is the density of the ambient water. Gebhart and Mollendorf (1977) show that for ambient temperature < 10°C salinity variations dominate density changes so that Eq. (9) becomes

$$B_d = g\beta\int_0^\infty (S_\infty - S)dy, \tag{10}$$

where $\beta = 1/\rho(\partial\rho/\partial s)$. With the theoretical results of Josberger (1979) Eq. (10) becomes

$$B_d = g\beta\Delta S\gamma z^{1/4}, \tag{11}$$

where ΔS is the difference between the ice-water interface salinity S_w, and the ambient salinity S_∞ and γ is a shape factor listed in Table 2. This shape

TABLE 2. Nondimensional shape factor.

T_d	γ
2	0.086
4	0.081
8	0.092

factor is the salinity deficit integrated across the turbulent boundary layer and is a function of the thermal driving T_d. The thermal driving is the temperature elevation above the freezing point of the salt water, defined as

$$T_d = T_\infty - T_{fp}, \tag{12}$$

where T_∞ is the farfield temperature and T_{fp} the freezing point of the farfield saltwater. The thermal driving is a convenient parameter to use in the ice melting problems because the melt rate equals zero when T_d equals zero.

5. Comparison of dilution and bubble buoyancies

To compute both B and B_d, I used the results of Gow (1968) and Josberger (1979) to provide values for the variables of Eqs. (8) and (11). Gow gives

$$r_1 = 0.5 \text{ mm} \quad \text{and} \quad N_i = 0.2 \text{ mm}^{-3} \tag{13}$$

and $d = 200$ m is a characteristic iceberg draft. Josberger (1979) gives σ as proportional to $z^{-1/4}$ and his experiments give the proportionality constant M_0 as

$$M_0 = 7.54 T_d^{1.63} \times 10^{-4} \text{ mm}^{5/4} \text{ s}^{-1}, \tag{14}$$

which on substitution into Eq. (8) and performing the integration gives

$$B = \frac{32\pi\nu}{3} r_1 \hat{p}^{1/3} N_i M_0 d^{3/4}. \tag{15}$$

Table 3 gives both B and B_d for $T_d = 2, 4, 8$°C with the distance from the bottom of the ice wall varying from 50 to 200 m. Both the bubble and dilution buoyancies increase with increasing T_d and d. For the antarctic case, $T_d < 4$°C and $d \approx 200$ m, the bubble buoyancy equals or exceeds the dilution buoyancy. For $T_d = 8$°C, the bubble buoyancy equals the dilution buoyancy when $d = 100$ m and it is approximately three times the dilution buoyancy when $d = 200$ m. Therefore, the release of air bubbles by the melting glacier ice may have a significant impact on melt driven convection for length scales > 100 m.

6. Laboratory experiments

To determine any additional bubble effects I performed two laboratory experiments using bubbly ice and then compared the results to those of Josberger (1979). The comparison shows for the bubbly ice case that the ice no longer melts in a smooth fashion and the ice-saltwater interface temperature is colder.

To produce ice with a suitable bubble content, I let 1 kg of dry ice sublimate in water at 0°C in a tank measuring 0.6 m × 0.4 m × 0.3 m which was in a variable temperature cold room. I then lowered the room temperature to −20°C and because the sides of the tank were insulated, the freezing began at the top of the tank and progressed downward. As the ice grew, the dissolved CO_2 was excluded from the crystalline ice structure and formed bubbles at the ice-water interface. These bubbles then froze into the ice block as the ice continued to grow. The bubbles had a characteristic diameter of 1 mm and a uniform distribution within the ice. I determined the CO_2 content by melting a known mass of ice in heated paraffin oil and collecting the CO_2 in a burrette.

I placed the ice slabs vertically in a tank that measured 1.2 m deep, 1.2 m long and 0.4 m wide which was filled with a NaCl solution at oceanic salinities. Josberger (1979) gives a complete description of the apparatus and experimental procedure. In the experiments I chose far-field conditions of $T_\infty = +2.4$°C, $S_\infty = 32.7$‰, or $T_d = 4.2$°C for the 5% CO_2 case and $T_\infty = +2.6$°C, $S_\infty = 33.5$‰, or $T_d = 4.4$°C for the 1.5% CO_2 case. I chose these conditions for comparison to the results of bubble-free ice experiments performed by Josberger (1979) at similar far-field conditions.

Compared to the bubble-free ice experiments, the bubbly ice melted in a rough irregular fashion. Fig. 1, from the 5% CO_2 case, shows the ice surface after melting for 1 h; the surface is pock-marked with irregular indentations. These indentations have characteristic depths and lengths of 5 and 30 mm and they continued to grow deeper and wider over the course of an experiment. Because of the irregular nature of the ablation I could only estimate the melt rate and these estimates lie within 10% of the values from the bubble-free experiments.

The ice-water interface temperature in the bubbly case is colder than in the bubble-free case which

TABLE 3. Bubble buoyancy and dilution buoyancy as a function of T_d and distance from the bottom of the ice wall.

Bubble buoyancy T_d (°C)				Dilution buoyancy T_d (°C)			
d (m)	2	4	8	d (m)	2	4	8
50	18.8	58.3	180.4	50	92.2	157.6	278.6
100	35.6	110.2	341.4	100	109.4	187.5	331.3
150	59.0	182.6	565.4	150	121.1	207.5	366.6
175	79.5	246.0	761.6	175	125.8	215.6	381.1
200	133.2	412.0	1275.4	200	130.1	222.9	394.0

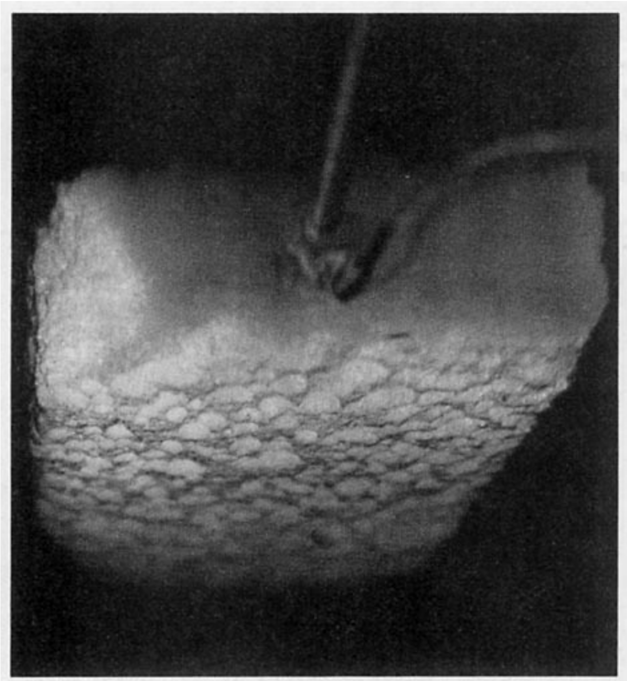

FIG. 1. Cusps in the ice after melting for 60 min, looking obliquely down at the ice from the top of the tank: T = 2.4°C and S = 32.7‰. The ice is 200 mm wide.

reduces the upward buoyant forcing. In this case, the colder T_w corresponds to a higher S_w which decreases the density difference driving the convective motions. For the 5% CO_2 case, I found a vertically uniform T_w of −1.35°C; for the bubble-free case I found a vertically uniform T_w of −0.80°C. Interface temperatures are not available from the other experiment due to failure of the data acquisition system.

In summary the effect of bubbles in the laboratory experiments is threefold. First, the ice melts in an irregular fashion. Second, the bubbles roughen the ice surface which increases the salt transport to the ice to decrease S_w. Third, the bubbles impart upward momentum to the water adjacent to the ice.

7. Conclusions

These calculations show that the bubble buoyancy B increases with both increasing vertical length scale and T_d. When compared to the dilution buoyancy, B_d, B exceeds B_d for vertical length scales of 200 m at T_d = 2°C, 160 m at T_c = 4°C and 100 m at T_d = 8°C. Hence, for antarctic icebergs with vertical length scale in excess of 200 m, the bubble buoyancy makes a significant contribution to the buoyancy driving the convective motions next to the ice. The laboratory experiments performed at a vertical length scale where B is insignificant compared to B_d show that the bubbles in the ice roughen the ice surface which increases the turbulent transport of salt and heat to the ice and decreases the upward buoyant forcing. With the decrease in buoyancy the melt rate is expected to decrease; however, the melt rate remains unchanged as a result of the bubble-related increased turbulent heat transport.

Acknowledgments. I thank Dr. Steve Neshyba for scientific discussions on this subject. Also, I thank both Dr. Seelye Martin for providing the laboratory facilities and Peter Kauffman for his help in performing the experiments. Finally, I acknowledge the support of the Arctic Program of the Office of Naval Research under Contracts 30-262-3149 and N00014-76-C-0234, Contribution M79-35 of the Department of Oceanography, Contribution 509 of the Department of Atmospheric Sciences, both of the University of Washington, Seattle.

REFERENCES

Batchelor, G. K., 1967: *An Introduction to Fluid Dynamics*. Cambridge University Press, 615 pp.

Gebhart, B., and J. C. Mollendorf, 1977: A new density relation for pure and saline water. *Deep-Sea Res.*, **24**, 831–848.

Gow, A. J., 1968: Bubbles and bubble pressures in Antarctic glacier ice. *J. Glaciol.*, **7**, 167–182.

Josberger, E. G., 1979: Laminar and turbulent boundary layers adjacent to melting vertical ice walls in salt water. Ph.D. thesis, University of Washington, Seattle, 185 pp.

Patterson, W. S. B., 1975: *The Physics of Glaciers*. Pergamon Press, 250 pp.